ANL-7609

Argonne National Laboratory

LABORATORY SIMULATIONS OF CLADDING-STEAM REACTIONS FOLLOWING LOSS-OF-COOLANT ACCIDENTS IN WATER-COOLED POWER REACTORS

by

James C. Hesson, Richard O. Ivins,
Richard E. Wilson, Kazuo Nishio,
and Charles Barnes, Jr.

Printed in the United States of America
Available from
Clearinghouse for Federal Scientific and Technical Information
National Bureau of Standards, U. S. Department of Commerce
Springfield, Virginia 22151
Price: Printed Copy $3.00; Microfiche $0.65

ANL-7609
Reactor Technology

ARGONNE NATIONAL LABORATORY
9700 South Cass Avenue
Argonne, Illinois 60439

LABORATORY SIMULATIONS OF CLADDING-STEAM REACTIONS FOLLOWING LOSS-OF-COOLANT ACCIDENTS IN WATER-COOLED POWER REACTORS

by

James C. Hesson, Richard O. Ivins,
Richard E. Wilson, Kazuo Nishio,
and Charles Barnes, Jr.

Reactor Engineering Division

January 1970

TABLE OF CONTENTS

	Page
ABSTRACT	7
I. INTRODUCTION	8
II. CLADDING-STEAM REACTION RATES	9
A. Zirconium-Steam Reaction	9
B. Stainless Steel-Steam Reaction	10
III. EXPERIMENTAL APPARATUS AND PROCEDURE	11
A. High-temperature Electrical-resistance Furnace	11
B. Induction-heated Assemblies	13
IV. RESULTS AND DISCUSSION	14
A. Tests in Electrical-resistance Furnace	14
1. Type 304 Stainless Steel-clad Fuel Rods	14
a. Test No. 1S	14
b. Test No. 2S	15
c. Tests No. 3S to 6S	17
2. Zircaloy-2-clad Fuel Rods	19
a. Test No. 1Z	19
b. Tests No. 2Z to 4Z	20
c. Test No. 5Z	22
d. Tests No. 6Z to 9Z	23
B. Tests in Induction-heated Assemblies	24
1. Meltdown of Zircaloy-2-clad Fuel Rods	24
a. Test No. 1Z-1	25
b. Test No. 1Z-2	25
2. Overall Effects of Water Quenching	26
3. Parametric Tests of Induction Heated-water Quenched Fuel Rods	27
4. Effects of Hydriding	31
V. CONCLUSIONS	37
REFERENCES	39

LIST OF FIGURES

No.	Title	Page
1.	High-temperature Electrical-resistance Furnace Used to Heat Fuel Rods in Steam at Temperatures and Pressures up to 1700°C and 1000 psig	12
2.	Temperature Distribution in Electrical-resistance Furnace during Test No. 1S	12
3.	Induction-heated Assembly	13
4.	Type 304 Stainless Steel-clad Fuel Rod before and after Exposure for 180 min to Steam at 1 g/min at 1500°C and 1 atm	15
5.	Hydrogen Evolution and Temperature Profile at Top End of Type 304 Stainless Steel-clad Fuel Rod during Exposure to Steam at 1600°C and 1 atm	16
6.	Type 304 Stainless Steel-clad Fuel Rod before and after Exposure for 10 min to Steam Flow of 10 g/min at 1600°C and 1 atm	16
7.	Photomacrographs near Top of Type 304 Stainless Steel-clad Fuel Rod Exposed in Test No. 2S	17
8.	Bundle of Four Type 304 Stainless Steel-clad Fuel Rods after Exposure for 10 min to Steam Flow of 25 g/min at 1600°C and 1 atm	18
9.	Zircaloy-2-clad Fuel Rod before and after Exposure for 270 min to Steam Flow of 1 g/min at 1500°C and 2 atm	20
10.	Hydrogen Evolution and Temperature Profile at Top End of Zircaloy-2-clad Fuel Rod during Exposure to Steam Flow of 10 g/min at 1600°C and 1 atm	21
11.	Appearance of Zircaloy-2-clad Fuel Rod before and after Exposure in Test No. 2Z	21
12.	Cross Section of Top Cap of Zircaloy-2-clad Fuel Rod after Exposure for 10 min to Steam Flow of 1 g/min at 1600°C and 1 atm	21
13.	Calculated Regional Rates of Reaction between Zircaloy-2 Cladding and Steam in Test No. 2Z	22
14.	Bundle of Four Zircaloy-2-clad Fuel Rods after Exposure for 10 min to Steam Flow of 25 g/min at Temperatures Greater Than 1700°C and 1 atm	23

LIST OF FIGURES

No.	Title	Page
15.	Effect of Steam Flowrates on Hydrogen Evolution from Zircaloy-2-clad Fuel Rods	24
16.	Oxide Ring Around Zircaloy-2-clad Fuel Rod Exposed to Limited Steam Flow at 1540°C and 1 atm	24
17.	Zircaloy-2-clad Fuel Rod Induction-heated in Steam to an Indicated Cladding Temperature of 2140°C	25
18.	Induction Heated-water Quenched Zircaloy-2-clad Fuel Rods in Order of Increasing Cladding Oxidation	32
19.	Selected Horizontal Cross Sections of Cladding Cut from Midpoint and Levels below Midpoint of Heated 3-in.-long Section of Zircaloy-2-clad Fuel Rods Exposed in Parametric Tests	33
20.	Heated Sections of Zircaloy-2-clad Fuel Rods Exposed to Hydrogen and Hydrogen-Steam Atmospheres in Tests No. H1 to H5	35
21.	Selected Horizontal Cross Sections of Cladding Cut from Midpoint and Levels below Midpoint of Heated 3-in.-long Section of Zircaloy-2-clad Fuel Rods Exposed in Tests No. H1 to H5	36

LIST OF TABLES

No.	Title	Page
I.	Reaction of Stainless Steel-clad Fuel Rods with Steam in Electrical-resistance Furnace	14
II.	Reaction of Zircaloy-2-clad Fuel Rods with Steam in Electrical-resistance Furnace	19
III.	Summary of Parametric Tests of Induction Heated-water Quenched Fuel Rods	29
IV.	Failure Pattern of Inductively Heated Single Zircaloy-2-clad Fuel Rods	30
V.	Summary of Hydriding Scoping Tests of Single Zircaloy-2-clad Fuel Rods	34

LABORATORY SIMULATIONS OF CLADDING-STEAM REACTIONS FOLLOWING LOSS-OF-COOLANT ACCIDENTS IN WATER-COOLED POWER REACTORS

by

James C. Hesson, Richard O. Ivins,
Richard E. Wilson, Kazuo Nishio,
and Charles Barnes, Jr.

ABSTRACT

Specimen Zircaloy-2-clad and Type 304 stainless steel-clad UO_2-pellet rods were electrically heated in steam and hydrogen-steam atmospheres to assess the damage that might be incurred in water-cooled reactor cores by a delay or failure in the operation of emergency core-cooling systems following loss of primary coolant.

It was observed that when oxidized in a steam atmosphere, Type 304 cladding foams and expands at temperatures approaching its melting point (~1400°C). Zircaloy-2 cladding is severely embrittled when the total oxygen absorbed is about 18% or greater (as ZrO_2). Zircaloy-2-clad UO_2-pellet fuel rods can be heated to about 1200°C in a steam atmosphere and then water-quenched without incurring sufficient oxidation and embrittlement to break on cooling. At temperatures substantially above 1200°C, the cladding tends to crack and break on cooling.

When exposed to pure hydrogen for 6 min, or longer, at 1400°C, Zircaloy-2 cladding is embrittled due to hydriding. Hydrogen embrittlement is reduced by preoxidizing the cladding in steam, or by the presence of steam in the hydrogen.

The effects of hydriding are adjudged secondary to those of steam oxidation, since conditions that might produce sufficient hydrogen embrittlement of the cladding in one core region would cause much greater embrittlement due to steam oxidation in other regions.

I. INTRODUCTION

Loss of primary coolant resulting from a rupture in the primary-system piping has served as the "design basis accident" for most water-cooled nuclear power reactors built to date in the U.S. During normal operation of these reactors, the primary coolant (either water or a water-steam mixture) removes heat from the core for steam generation or other purposes. Upon loss of this coolant, because of a pipe break or other reasons, the reactor is shut down (nuclear) and emergency core-cooling systems (ECCS), such as in-core water-spray or -flooding devices are actuated to remove fission-product decay-heat energy from the fuel. However, since this energy continues to heat the core rapidly after nuclear shutdown, the temperature rise may be sufficient to damage the fuel cladding (and the fuel) in case of a delay in effective ECCS operation. The damage may be incurred by: (1) oxidation or oxygen absorption due to reaction between the cladding and steam from residual water; (2) hydriding or absorption of hydrogen evolved from the cladding-steam reaction; (3) reaction between the cladding and the fuel; (4) melting of the cladding; or (5) straining, warping, swelling, or bursting of the cladding due to internal pressures.

Accordingly, a series of out-of-pile tests was conducted, using single UO_2 fuel rods and bundles of four to assess the extent of damage and failure of the cladding and fuel as a function of simulated loss-of-coolant conditions, including failure or delay in ECCS operation. In the early tests, the fuel rods were exposed to steam at various temperatures and flowrates in an electrical-resistance furnace. In subsequent tests, the rods were heated inductively in a flowing-steam atmosphere. In a number of cases, these rods were quenched at a predetermined temperature, either by spraying water from the top or by flooding from the bottom, to simulate emergency cooling. Zircaloy-2-clad rods were used in most of the tests; however, some of the early tests were conducted using Type 304 stainless steel-clad rods. Finally, Zircaloy-2-clad rods were also inductively heated in a hydrogen atmosphere to investigate the relative damage as compared to heating in a steam atmosphere.

The progress of these tests was reported in Argonne Chemical Engineering Division Semiannual Reports.[1-7] This report is a summary of the nature and findings of these tests. Briefly, these findings were:

1. When oxidized by heating in a steam atmosphere, Type 304 stainless steel cladding foams and expands at temperatures approaching its melting point (~1400°C).

2. Zircaloy-2 cladding is embrittled, and the degree of embrittlement increases with the amount of oxygen absorbed. The cladding becomes very brittle when the total oxygen absorbed is about 18% or greater (as ZrO_2).

3. Zircaloy-2-clad, UO_2-pellet rods can be heated in a steam atmosphere to about 1200°C and then water-quenched without undergoing sufficient oxidation and embrittlement to break on cooling. At temperatures substantially above 1200°C, the cladding tends to crack and break on cooling.

4. The effects of hydriding on Zircaloy-2 cladding are secondary to those of oxidation.

II. CLADDING-STEAM REACTION RATES

When heated in steam or water vapor, Zircaloy-2 and stainless steel cladding can react with the steam to form metal oxides and hydrogen. Since Zircaloy-2 is composed primarily of zirconium, its reaction rate is very nearly the same as that of zirconium.

The following information has been extracted from studies of reaction rates of zirconium with steam and stainless steel with steam.[8-11]

A. Zirconium-Steam Reaction

Baker and Just[10] have reported that when the steam is in excess at the reacted surface, the reaction of zirconium cladding with the steam follows a parabolic rate law. For a cylindrical surface, the rate is given by

$$\frac{d(r_0 - r)}{dt} = \frac{K}{r_0 - r} \exp(-\Delta E/RT) \text{ cm/sec}, \qquad (1)$$

where

r = radius of unreacted metal in rod, cm;

r_0 = original radium of unreacted metal, cm;

t = time, sec;

ΔE = activation energy = 45,500 cal/mole;

K = rate law constant = 0.3937 cm^2/sec;

R = gas constant = 1.987 cal/(mole)(°K);

and

T = cladding temperature, °K.

Here $r_0 - r$ represents a thickness of oxidized metal which retards the reaction in proportion to its thickness.

At relatively high temperatures, the reaction becomes more rapid and may be limited by the diffusion of steam to the oxide surface and the diffusion of hydrogen from the oxide surface. In this case,

$$\frac{d(r_0 - r)}{dt} = \frac{\rho_g M_c}{\rho_c} h_d (X - X_s) \text{ cm/sec}, \qquad (2)$$

where

ρ_g = density of the gas (steam-hydrogen mixture), moles/cm^3;

ρ_c = density of the cladding = 6.5 g/cm^3;

M_c = grams cladding oxidized per mole steam = 45.6 g/mole;

X = average concentration of steam in gas, moles/mole;

X_s = concentration of steam in gas at reacted surface (assumed very small, i.e., $X - X_s = X$), moles/mole;

and

h_d = mass-transfer coefficient for steam through hydrogen or hydrogen through steam, cm/sec

$= D_g/\sigma_d$,

where

σ_d = effective gas film thickness for diffusion, cm

and

D_g = diffusivity of hydrogen in steam, cm^2/sec.

When 1 g of zirconium is oxidized in steam, about 1550 cal of heat are released.

B. Stainless Steel-Steam Reaction

Although the reaction of stainless steel with steam has been studied,[4,11] a theoretically based rate law, which adequately describes the reaction over a specific temperature range, has not been developed.

Early calculations for loss-of-coolant accidents assumed that the reaction rate is very low until the metal temperature reaches 1400°C (1673°K, or slightly above its melting point), whereupon the rate is limited

by diffusion of steam to the reacting surface. In the reaction, 0.51 liter of hydrogen (0.0227 mole) is evolved from the reaction of water vapor with 1 g of stainless steel. Thus

$$\frac{d(r_0 - r)}{dt} = 0 \tag{3}$$

at $T < 1400°C$, and

$$\frac{d(r_0 - r)}{dt} = \frac{\rho_g M_c}{\rho_c} h_d(X - X_s) \tag{4}$$

at $T > 1400°C$, where

$$\rho_c = 8 \text{ g/cm}^3,$$

and

$$M_c = 44 \text{ g/mole}.$$

More recently it has been stated[11] that the reaction of stainless steel with steam follows a parabolic rate law, the same as for zirconium. Rate-law constants were determined to be

$$K = 1.41 \times 10^6 \text{ cm}^2/\text{sec}$$

and

$$\Delta E = 90800 \text{ cal/mole}.$$

In this case, Eq. 1 could be used for the kinetic (nonsteam-limited) condition at temperatures below 1400°C.

When 1 g of Type 304 stainless steel is oxidized in steam, about 254 cal at 1327°C (solid states) or 155 cal at about 1400°C (molten states) are released.

III. EXPERIMENTAL APPARATUS AND PROCEDURE

A. High-temperature Electrical-resistance Furnace

The furnace used in the early experiments is designed for temperatures and pressures up to 1700°C and 1000 psig. As shown schematically in Fig. 1, it consists of an inner, steam-filled zone enclosed by an alumina tube, and an outer, argon-filled zone enclosed by a steel pressure vessel.

The upper part of the argon zone contains molybdenum heater windings and insulation; these are wrapped around and identify the high-temperature zone of the alumina tube.

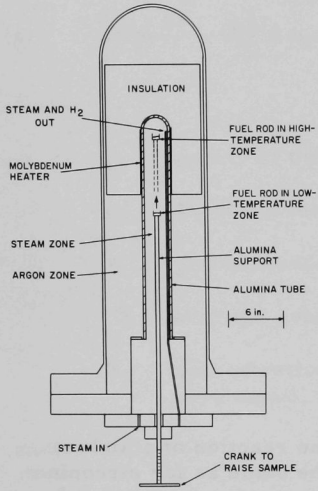

Fig. 1. High-temperature Electrical-resistance Furnace Used to Heat Fuel Rods in Steam at Temperatures and Pressures up to 1700°C and 1000 psig. ANL Neg. No. 108-7179 Rev. 1.

Preparatory to each experiment, the molybdenum heater is energized and the furnace is brought to operating temperature. A single fuel rod (or bundle of four rods) is installed vertically in the alumina holder, which is positioned in the lower (cooler) section of the alumina tube. The tube is purged with argon, and the furnace is brought up to operating pressure.

Water is introduced by a positive displacement pump into the lower part of the steam zone, where it is converted into steam. Some unreacted steam and the hydrogen evolved from the metal-steam reaction are removed continuously through an outlet tube in the high-temperature section of the steam dome. The extent of the reaction is determined from the amount of hydrogen collected. Pressure in the steam zone and argon zone is automatically regulated and matched to avoid stresses in the alumina tube.

After conditions have stabilized, the alumina holder and the fuel rod are raised, by an external crank mechanism, into the upper (hottest) part of the steam zone to simulate decay heating. Furnace interior and fuel cladding temperatures are monitored by alumina-insulated Pt/Pt-Rh10 thermocouples. Figure 2 shows a typical temperature distribution in the furnace (in this case, test No. 1S).

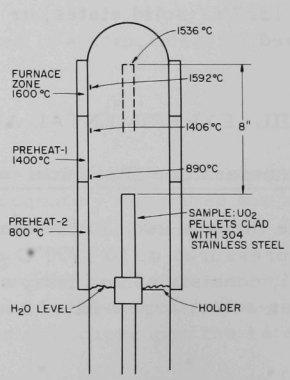

Fig. 2

Temperature Distribution in Electrical-resistance Furnace during Test No. 1S. ANL Neg. No. 108-8575.

B. Induction-heated Assemblies

Two types of assemblies were used: one (Fig. 3a) for simulating a loss-of-coolant accident, and the other (Fig. 3b) for simulating a loss-of-coolant accident followed by water quenching (simulated emergency cooling). Basically, each assembly consisted of a single fuel rod (or bundle of four rods) mounted in a quartz tube. Single rods were heated in a 0.865-in.-ID tube. When a bundle of four rods was heated, a $1\frac{9}{16}$-ID tube was used. Steam was admitted at the bottom of the tube, and the hydrogen evolved and the residual steam or water were removed at the top.

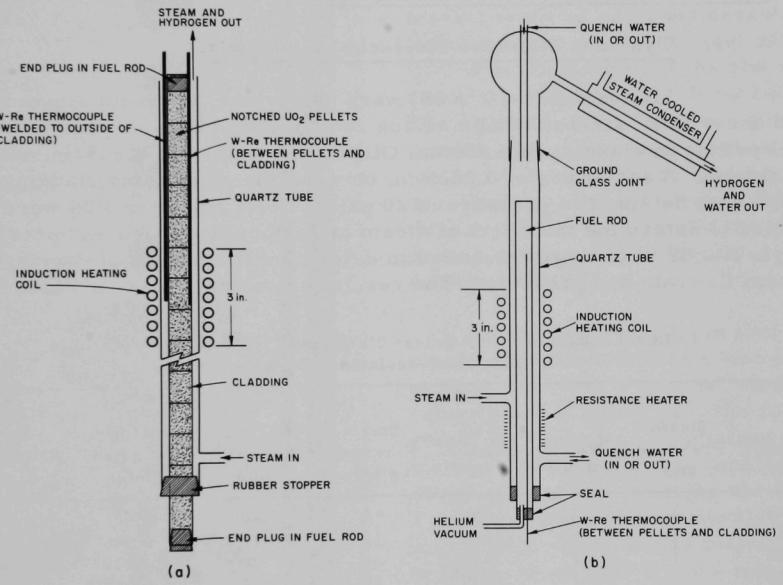

Fig. 3. Induction-heated Assembly. (a) As used to simulate loss-of-coolant accident; (b) as modified to include water quenching (simulated emergency cooling).

For experiments designed to simulate emergency cooling, the assembly was modified as shown in Fig. 3b. With this arrangement, quench water could be injected at either the top or bottom of the tube and removed at the opposite end. An electrical-resistance heater was wrapped around the bottom of the tube to prevent steam condensation at this location. A water-cooled condenser was installed at the top of the tube to condense steam from the effluent hydrogen. The hydrogen was collected and its volume measured by displacing water from graduated cylinders. Samples of the gas were analyzed to check for air leakage into the system.

Cladding temperatures were monitored by beryllia-insulated, tantalum-clad W5-Re/W26-Re thermocouples. These were held against the interior surface of the cladding by notches in the UO_2 pellets. Similar thermocouples were welded to the exterior surface, but the steam atmosphere caused their early failure. Thus, in some tests, an optical two-color pyrometer was used to measure exterior surface temperatures.

IV. RESULTS AND DISCUSSION

A. Tests in Electrical-resistance Furnace

1. Type 304 Stainless Steel-clad Fuel Rods

Six tests (No. 1S to 6S) were performed, five with single rods and one with a four-rod bundle. Each rod consisted of high-density UO_2 fuel pellets in cladding of 0.426-in. OD, 8-in. length, and 0.025-in. wall thickness. A radial gap of 0.0025 in. between the pellets and cladding was filled with helium at a pressure of 20 psia. Tests No. 1S and 2S were conducted to determine the effect of steam at various flowrates and pressures. Tests No. 3S to 6S were conducted to determine the effects of varying both steam flowrate and pressure. The results are summarized in Table I.

TABLE I. Reaction of Stainless Steel-clad Fuel Rods with Steam in Electrical-resistance Furnace

Exp. No.	Steam Pressure, atm	No. of Rods	Rod Temp,[a] °C	Steam Flowrate, g/min	Duration of Test,[b] min	Hydrogen Collected, moles	Stainless Steel Oxidized,[c] %
1S	2	1	1500	~1	180	0.401	44.2
2S	1	1	1600	10	10	0.346	37
3S	1	1	1600	20	20	0.324	35.7
4S	4	1	1600	10	10	0.250	27.4
5S	11	1	1600	10	10	0.320	35.2
6S	1	4	1600	25	10	~1.32	~35

[a] At hottest area.

[b] Rods elevated into hottest furnace zone over 8-min period, maintained there, and rapidly withdrawn at end of test time.

[c] Based on 0.0228 mole (0.51 liter) of hydrogen per gram of stainless steel.[4]

a. Test No. 1S. With reference to Fig. 2, the center of the furnace zone was heated to 1536°C before the fuel rod was raised into the upper position. At this time, the top of the rod was at about 800°C. The rod was raised at a rate of 1 in./min. After insertion of the rod, the temperature at the center of the furnace zone dropped to 1488°C and then rose to 1499°C over a period of 12 min. Both thermocouples attached to the outer, upper surface of the cladding failed after 21 min. At the time of failure, the indicated temperature at the center of the hot zone was 1495°C.

The reaction was allowed to continue for 180 min from the time the rod was first inserted into the hot zone. Then the rod was lowered to its original position. About 0.401 mole or 9 liters (STP) of hydrogen were collected, mostly during the first 90 min. This amount of hydrogen corresponds to a reaction of about 44.2% of the stainless steel.

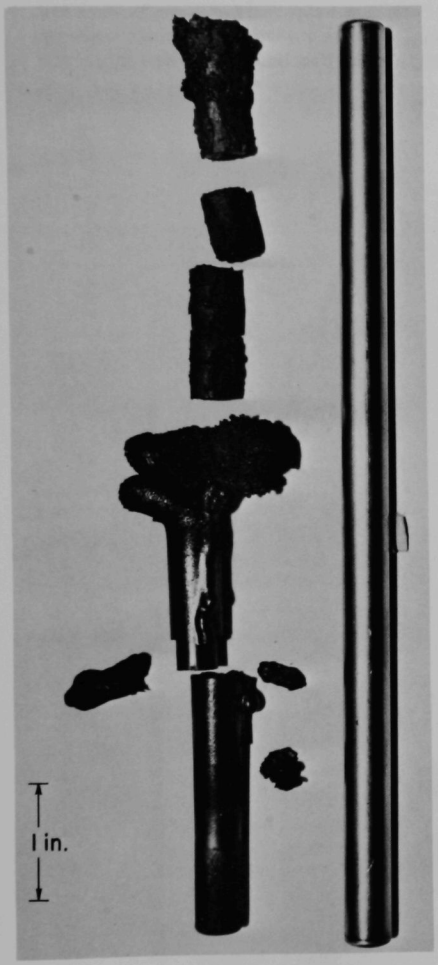

Fig. 4. Type 304 Stainless Steel-clad Fuel Rod before and after Exposure for 180 min to Steam at 1 g/min at 1500°C and 1 atm (test No. 1S). ANL Neg. No. 108-8018.

Figure 4 shows the fuel rod after removal from the furnace; also shown is an unreacted rod. Relatively little reaction occurred at the lower end of the rod, but extensive reaction and considerable foaming of the stainless steel occurred in the portion of the rod that reached a temperature above 1400°C. The cladding was almost completely removed from the upper portion of the fuel rod; the spongy mass is probably the remains of the 3/16-in.-thick top end cap. Some of the UO_2 pellets evidenced considerable deterioration.

b. Test No. 2S. In test No. 2S, the steam flowrate was set at 10 g/min, with a nominal steam velocity of 3.2 ft/sec past the rod; steam pressure was maintained at 1 atm. Total time of reaction with steam was 10 min. During the first 8 min, the fuel rod was elevated into the hot zone. It was maintained in that zone at 1600°C for 2 min and then withdrawn rapidly into the cooler section of the furnace. As shown in Fig. 5, the top of the fuel rod reached a maximum temperature of 1600°C and the bottom a maximum of 900°C, thereby creating an axial temperature drop of 700°C. The total hydrogen evolved corresponded to a reaction of 37% of the stainless steel cladding.

Figure 6 shows the rod before and after testing. The top one-third of the cladding appeared

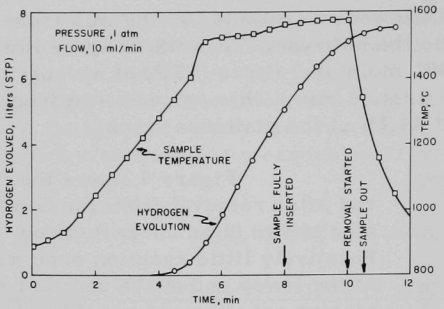

Fig. 5

Hydrogen Evolution and Temperature Profile at Top End of Type 304 Stainless Steel-clad Fuel Rod during Exposure to Steam at 1600°C and 1 atm (test No. 2S). ANL Neg. No. 108-8845 Rev. 1.

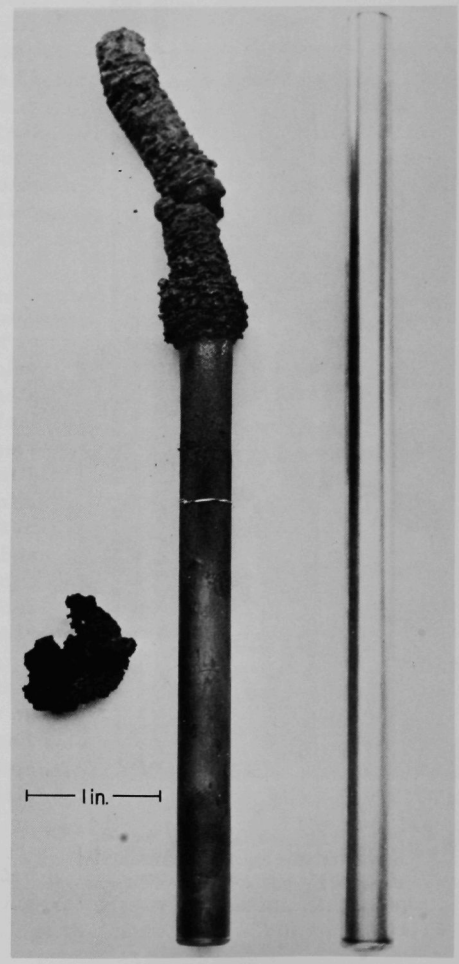

Fig. 6

Type 304 Stainless Steel-clad Fuel Rod before and after Exposure for 10 min to Steam Flow of 10 g/min at 1600°C and 1 atm (test No. 2S). ANL Neg. No. 108-8757 Rev. 1.

to be completely reacted, whereas the remainder had reacted slightly. Based upon results from other experiments,[1,4] the maximum temperature at the demarcation between the two reaction zones was estimated to be about 1400°C.

Metallographic examination of cross sections near the top of the fuel rod revealed areas of interaction between the UO_2 and the stainless steel oxides. These areas are shown in Fig. 7. The foamy appearance of the oxidized stainless steel is also apparent. X-ray analysis of the oxides revealed a γ-Fe_3O_4 -type structure.

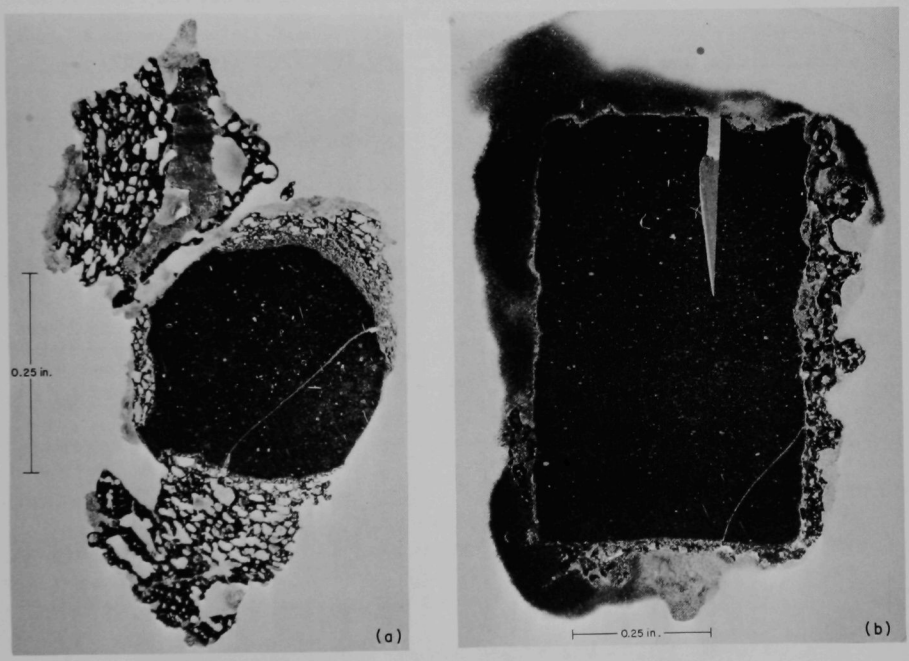

Fig. 7. Photomacrographs near Top of Type 304 Stainless Steel-clad Fuel Rod Exposed in Test No. 2S. (a) Radial cross section; (b) axial cross section. ANL Neg. No. (a) 108-8871; (b) 108-8870.

c. Tests No. 3S to 6S. As mentioned earlier, tests No. 3S to 6S were made to determine the effects of varying both the steam flowrate and pressure. In test No. 3S, the water flowrate was increased to 20 g/min and the pressure was maintained at 1 atm. In tests No. 4S and 5S, the flowrate was decreased to 10 g/min and the pressure was increased to 4 and 11 atm, respectively. The results (Table I), indicate that neither the rate nor the extent of stainless steel-steam reaction was significantly affected by the changes in steam flowrate or pressure.

In test No. 6S four rods in a square array with 0.6-in. center-to-center spacing were exposed to steam at 1600°C and 1 atm. Steam flow was maintained at 25 g/min to ensure that the reaction was not steam-limited. Other conditions were not altered from those used in the single-rod tests.

Figure 8a is an overall view of the four-rod bundle as removed from the furnace. Figure 8b is a close-up view of the areas of rapid "frothing" action and slow "corrosion" reaction which were at about 1400°C. In the area of rapid reaction, expansion of reaction products into the steam flow channel is evident, with some bridging between fuel rods.

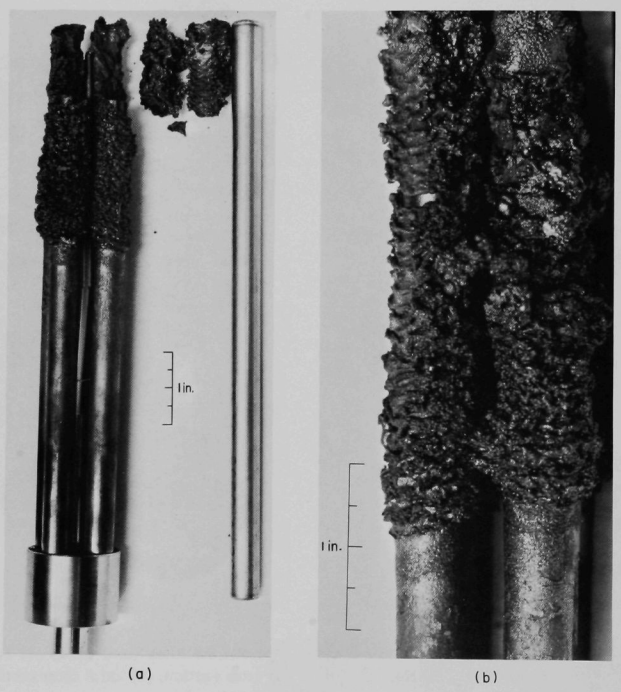

Fig. 8. Bundle of Four Type 304 Stainless Steel-clad Fuel Rods after Exposure for 10 min to Steam Flow of 25 g/min at 1600°C and 1 atm (test No. 6S). (a) Overall view with unexposed rod included for comparison; (b) close-up of rapid "frothing" and slow "corrosion" reaction areas. ANL Neg. No. (a) 108-9704; (b) 108-9705.

The total amount of hydrogen evolved was approximately four times that evolved in tests with single rods.

2. Zircaloy-2-clad Fuel Rods

Nine tests (No. 1Z to 9Z) were performed, eight with single rods and one with a four-rod bundle. Each rod consisted of high-density UO_2 fuel pellets in cladding of 0.426-in. OD, 8-in. length, and 0.027-in. wall thickness. A radial gap of 0.0025 in. between the pellets and cladding was filled with helium at a pressure of 20 psia. The test conditions and results are summarized in Table II.

TABLE II. Reaction of Zircaloy-2-clad Fuel Rods with Steam in Electrical-resistance Furnace

Exp. No.	Steam Pressure, atm	No. of Rods	Rod Temp,[a] °C	Steam Flowrate, g/min	Duration[b] of Test, min	Hydrogen Collected, moles		Zircaloy-2 Oxidized, %
1Z	2	1	1500	~1	270	0.371		52
2Z	1	1	1600	10	10	0.132	(0.152)[c]	18.5 (21.3[c])
3Z	4	1	1600	10	10	0.147		20.6
4Z	11	1	1600	10	10	0.113[d]		15.8[d]
5Z	1	4	1700	25	10	1.16		40.6
6Z	1	1	1540	2.5	10	0.0423	0.0486[e]	
7Z	1	1	1540	2.5	10	0.0409	0.0479[e]	
8Z	1	1	1540	0.25	10	0.0431	0.0490[e]	
9Z	1	1	1540	0.25	10	0.0419	0.0485[e]	

[a] At hottest area.
[b] Rod elevated into hottest furnace zone over 8-min period, maintained there, and rapidly withdrawn at end of test time.
[c] Value calculated from test temperature-time history for 1 atm and parabolic rate law.
[d] Low value due to slightly lower temperature reached during experiment.
[e] Hydrogen collected at end of 12 min.

a. Test No. 1Z. Except for the reaction time (270 min total), the Zircaloy-2-clad fuel rod was exposed to the same environment as was the Type 304-clad rod in test No. 1S. The total hydrogen collected corresponded to 52% reaction of the Zircaloy-2.

Figure 9 shows the rod before and after exposure. The upper two-thirds (hottest portion) of the cladding was completely reacted, forming a tube of ZrO_2 which retained the original shape of the metal. The oxide appeared to have considerable strength. Upon complete oxidation, the original diameter of the rod (0.426 in.) increased to between 0.458 and 0.486 in. In the broken sections, the cladding residue consisted of a white outer layer and a yellow inner layer.

The lower (cooler) portion of the cladding was slightly reacted. Most of the reaction occurred during the first 2 hr of exposure. It was apparent that the low steam flowrate had limited the rate of reaction.

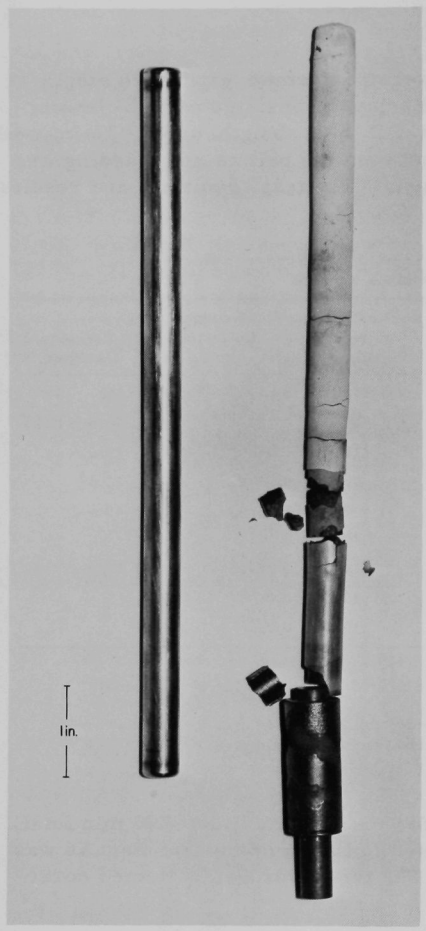

Fig. 9. Zircaloy-2-clad Fuel Rod before and after Exposure for 270 min to Steam Flow of 1 g/min at 1500°C and 2 atm (test No. 1Z). ANL Neg. No. 108-8059 Rev. 1.

b. Tests No. 2Z to 4Z. In tests, No. 2Z to 4Z, single rods were exposed for 10 min to 1600°C steam at 10 g/min and pressures of 1, 4, and 11 atm, respectively.

Figure 10 shows the temperature-time history of the top (hottest) end of the rod in test No. 2Z. As in test No. 2S, the top and bottom ends of the rod reached maximum temperatures of 1600 and 900°C, respectively, resulting in an axial temperature drop of 700°C. Measurements of the hydrogen evolved, also plotted in Fig. 10, indicated an overall reaction of 18% of the Zircaloy-2 cladding.

Figure 11 shows the appearance of the rod before and after test. The upper (hottest) end of the rod was embrittled, but only the outer surface of the cladding was converted to ZrO_2. Measurements made on a photomacrograph of a cross section of the top cap (Fig. 12) indicated a 0.014-in.-thick layer of cladding metal and an equal thickness of oxide film (original cladding wall thickness, 0.027 in.). There was no apparent interaction between the cladding and the UO_2 fuel, and no sharp demarcation between reaction zones; however, the attack on the cladding was more severe at the upper end than at the lower end.

As a check, the parabolic oxidation law was used to calculate the rate and extent of reaction of the fuel rod. Briefly, Eq. 1 was programmed on the CDC-3600 digital computer, using small time intervals. Arbitrary temperature-time functions could be inserted into the calculation. These functions are plotted in Fig. 13 and represent the approximate temperature history of various regions of the Zircaloy-2 cladding. Also plotted are the corresponding calculated reaction rates for these regions; these are expressed in terms of the mils of cladding reacted during the exposure.

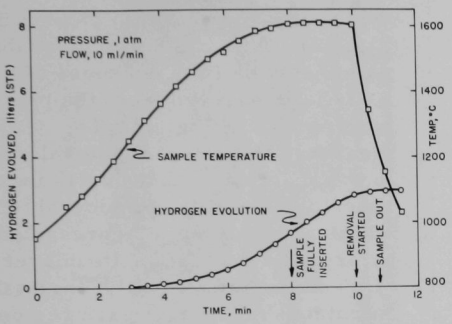

Fig. 10. Hydrogen Evolution and Temperature Profile at Top End of Zircaloy-2-clad Fuel Rod during Exposure to Steam Flow of 10 g/min at 1600°C and 1 atm (test No. 2Z). ANL Neg. No. 108-8846 Rev. 1.

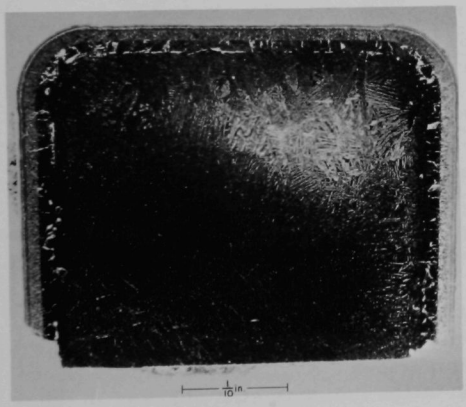

Fig. 12. Cross Section of Top Cap of Zircaloy-2-clad Fuel Rod after Exposure for 10 min to Steam Flow of 1 g/min at 1600°C and 1 atm (test No. 2Z). ANL Neg. No. 108-8868 Rev. 1.

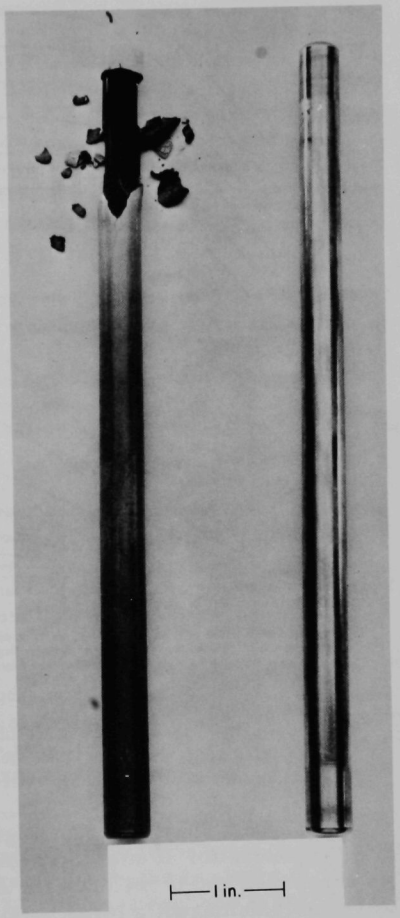

Fig. 11. Appearance of Zircaloy-2-clad Fuel Rod before and after Exposure in Test.No. 2Z. ANL Neg. No. 108-8758 Rev. 1.

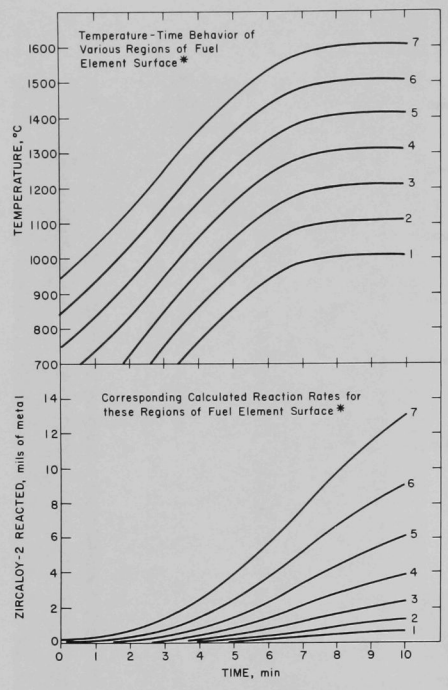

*Region 1, lowest 15.9% of surface; Region 2, 12.2% of surface; Region 3, 10% of surface; Region 4, 11.1% of surface; Region 5, 13.0% of surface; Region 6, 17.3% of surface; and Region 7, upper 20.5% of surface.

Fig. 13. Calculated Regional Rates of Reaction between Zircaloy-2 Cladding and Steam in Test No. 2Z. ANL Neg. No. 108-9419.

The amount of cladding reacted at the top (hottest) region of the fuel rod was calculated to be 0.0131 in. (see uppermost curve in Fig. 13). This compares favorably with the oxide film thickness of 0.014 in. measured from the photomacrograph in Fig. 12. The measured thickness is equivalent to the reaction of about 0.010 in. of Zircaloy; however, considerable additional reaction is represented by oxygen dissolved in a sublayer of α-zirconium. Finally, the total calculated reaction of each region of surface was summed over the seven regions, and the total hydrogen evolved and percent reaction for the entire fuel rod were calculated. As shown in Table II, the calculated extent of reaction was 0.152 mole of hydrogen (21.3% reaction), or only 15% higher than the measured value of 0.132 mole of hydrogen (18.5% reaction).

The fuel rods exposed in tests No. 3Z and 4Z were similar in appearance. There was no significant effect of increased pressure on either the rate or the extent of the Zircaloy-2-steam reaction.

c. Test No. 5Z. Figure 14 shows the bundle of four rods after exposure for 10 min to steam flow of 25 g/min at >1700°C and 1 atm. An unexposed rod is included for comparison. Although the exposed rods were badly damaged, a large portion of the fuel was still encased in tubes of oxidized Zircaloy-2. (Note: Some of the damage to the cladding occurred during removal of the test section from the furnace.)

Self-heating of the rods was apparent: During the test, the indicated temperature at the upper (hottest) end of the bundle was more than 200°C above the furnace temperature of 1700°C. This self-heating is attributed to thermal isolation in the four-rod bundle.

Hydrogen evolution per fuel rod was about twice that evolved in the single-rod tests. This was expected because of the higher temperatures reached by the four-rod bundle.

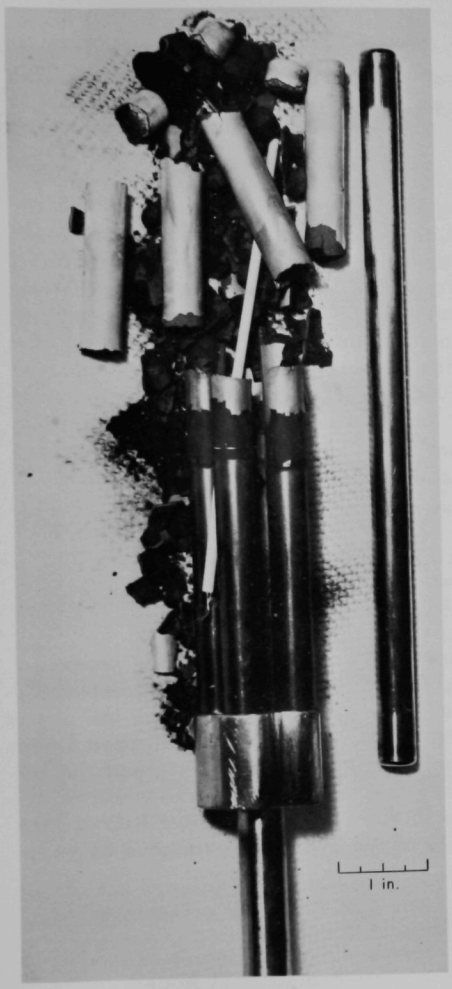

Fig. 14. Bundle of Four Zircaloy-2-clad Fuel Rods after Exposure for 10 min to Steam Flow of 25 g/min at Temperatures Greater Than 1700°C and 1 atm (test No. 5Z). ANL Neg. No. 108-9257-A.

d. Tests No. 6Z to 9Z. In tests No. 6Z to 9Z, single rods were exposed for 10 min to flowing steam at 1540°C and 1 atm. In tests No. 6Z and 7Z, the steam flowrate was maintained at 2.5 g/min; in tests No. 8Z and 9Z, it was maintained at 0.25 g/min. In all tests, the hydrogen evolved was collected for an additional 2 min after the rod was withdrawn from the hot zone.

With regard to the steam flowrate, although different amounts of water were metered into the furnace, there is no way of measuring the amount of steam flow past the fuel rod. Convection currents of steam are established because of the relatively large reaction chamber ~2-in. ID) compared to the size of the steam exit tube (1/8-in. ID). However, based upon the data, it is concluded that the steam flow past the hot fuel rod remained relatively constant during each test.

Figure 15 shows that the total hydrogen evolved during these tests was about one-third that evolved during test No. 2Z in which there was excess steam.

Another observation made during these tests with limited steam flowrates is shown in Fig. 16. This rod was exposed in test No. 6Z. The ring of white oxide (see inset) is believed to have been caused by a combination of an axial temperature gradient (hotter at the top), which would promote reaction at the upper end, and the limited steam, which would promote reaction toward the lower end of the rod. Location of greatest reaction is therefore centered at a point below the top of the rod. In tests with a high steam flowrate, the greatest reaction has occurred at the top (hottest point) of the rod.

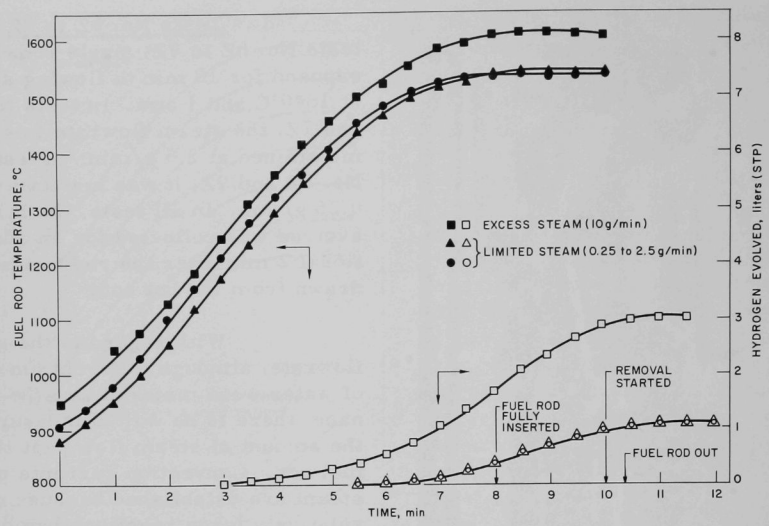

Fig. 15. Effect of Steam Flowrates on Hydrogen Evolution from Zircaloy-2-clad Fuel Rods (furnace temperature = 1500°C; pressure = 1 atm). ANL Neg. No. 308-543 Rev. 1.

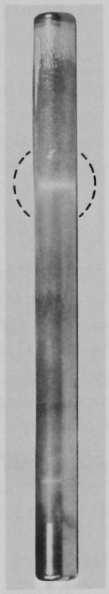

This observation suggests that in a power-reactor loss-of-coolant accident, chemical reaction between the fuel rods and steam would begin at a point below the center (hottest point) of the reactor under conditions of limited steam availability. As the temperature increased throughout the reactor core because of decay heating, the reaction would propagate to still lower regions of the core. The upper half of the core would be exposed only to the hydrogen produced by reaction at the lower positions.

B. Tests in Induction-heated Assemblies

1. Meltdown of Zircaloy-2-clad Fuel Rods

Two meltdown tests were conducted, one with a single fuel rod (test No. 1Z-1) and the other with a bundle of four rods (test No. 1Z-2). Each rod consisted of high-density UO_2 fuel pellets in cladding having 0.426-in. OD, 8-in. length, and 0.027-in. wall thickness. In addition, each rod was filled with helium at a pressure of 20 psia.

Fig. 16. Oxide Ring around Zircaloy-2-clad Fuel Rod Exposed to Limited Steam Flow at 1540°C and 1 atm (test No. 6Z). ANL Neg. No. 108-9890 Rev. 2.

a. Test No. 1Z-1. The objective of test No. 1Z-1 was to observe some of the features of the meltdown and collapse of a single fuel rod. As shown in Fig. 3a, the rod was positioned in a quartz steam jacket, which, in turn, was surrounded by a 3-in.-long induction-heating coil near the center. Steam flowrate was maintained at 1 g/min.

Fuel-rod temperatures were to be measured by two W5-Re/W26-Re thermocouples, one positioned between the fuel pellets and the cladding, and the other welded to the outer surface of the cladding. However, the thermocouple recordings could not be interpreted because of interference from the rf field generated by the induction-heating coil. A temperature record was obtained using a Pyroeye two-color pyrometer, which was focused on the cladding surface between turns of the induction-heating coil. During the test, this record, which was limited to the high range of the instrumented (1900-2500°C), indicated a peak temperature of 2140°C. Power to the coil was turned off a few seconds after the temperature peaked.

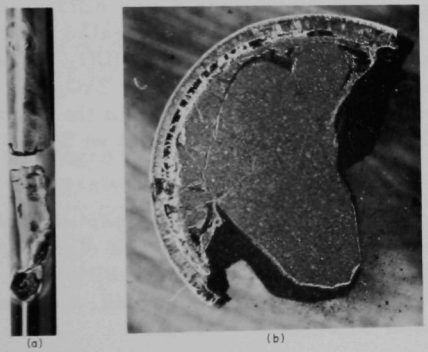

Fig. 17. Zircaloy-2-clad Fuel Rod Induction-heated in Steam to an Indicated Cladding Temperature of 2140°C (a) External Appearance; (b) Cross Section near Center. ANL Neg. No. 308-540.

Although preliminary in nature, this test showed there was no tendency for the molten Zircaloy to drop from the fuel rod. Rather, as shown in Fig. 17a, it was confined between an outer "crucible" of zirconium oxide and the inner surface of the UO_2. Also, as shown in the cross section (Fig. 17b), there was evidence of interaction between the molten Zircaloy and UO_2, and local melting of the UO_2. These observations support the contention that fuel-rod breakup in tests No. 2Z and 5Z occurred during the cool-down phase and was not inherent in the high-temperature failure process.

b. Test No. 1Z-2. A true simulation of loss-of-coolant-accident conditions requires a large number of fuel rods to achieve a realistic thermal environment for each rod. Accordingly, four Zircaloy-2-clad fuel rods were induction-heated simultaneously in test No. 1Z-2.

These rods were assembled on 0.6-in. centers in a square lattice by means of Teflon end plugs. Two W5-Re/W26-Re thermocouples were positioned between the grooved UO_2 pellets and the cladding, one facing the center of the bundle and the other facing the perimeter. This assembly was then installed inside a quartz steam jacket ($1\frac{9}{16}$-in. ID).

As in test No. 1Z-1, a 3-in.-long induction-heating coil was wrapped around the central region of the jacket.

During this test, the steam flowrate was maintained at 4 g/min (1 g/(min)(rod)). Both thermocouples peaked at 1800°C after 80 sec of heating. Ten seconds later, the thermocouple facing the center of the bundle indicated a sharp rise to 2950°C, while the other one (facing the perimeter) registered a decrease to about 1450°C. (Note: The sharp rise in temperature may have been caused by molten UO_2 contacting the thermocouple and then falling away.) Color films of the test confirmed the uneven temperature distribution. They showed that hot zones occurred in areas adjacent to another rod; i.e., there was a large temperature gradient from the inner side of the rods to the outer side. The inner thermocouple was located in one of these hot zones.

Upon removal of the assembly, visual examination revealed extensive, longitudinal rupture of the cladding in areas adjacent to another rod, and evidence of molten UO_2. (Note: The consensus was that fragmentation occurred after the test was terminated.) Subsequent X-ray diffraction examination of a 0.25-in.-dia droplet from a ruptured area revealed a face-centered-cubic phase with lattice parameters of 5.28 to 5.31 Å (UO_2, 5.470 Å; ZrO_2, 5.10 Å), thus indicating a solid solution between ZrO_2 and UO_2. Electron microprobe analysis of a similar particle showed the presence of mixed uranium-zirconium oxides, which varied from 34 wt % U-33 wt % Zr to 24 wt % U-43 wt % Zr.

The temperature gradient observed between inner and outer edges of each rod, and the subsequent longitudinal rupture of the cladding along the inner walls of the four-rod bundle, indicate the desirability for additional experiments using more rods per bundle--for example, a center rod with at least one, and preferably two, outer rows of rods.

2. Overall Effects of Water Quenching

Three tests (No. 1Z-4, 1Z-5, and 1Z-6) were conducted with single Zircaloy-2-clad rods to determine the gross overall effects of inductively heating the rods in flowing steam and then suddenly quenching the rods by a water spray from the top to simulate emergency cooling. The test apparatus is shown in Fig. 3b.

In each test, the fuel rod consisted of high-density UO_2 fuel pellets in Zircaloy-2 cladding of 0.426-in. OD, 8-in. length, and 0.027-in. wall thickness. Two W5-Re/W26-Re thermocouples were used to measure fuel-rod temperatures: One was positioned in a groove between the UO_2 pellets and the cladding; the other was spot-welded to the outer surface of the cladding. Each rod was then filled with helium at a pressure of 20 psia.

Each rod was exposed to steam at a flowrate of 1 g/min and inductively heated to a temperature near the melting point of Zircaloy-2 (~1850°C). At that time, water was sprayed into the top of the quartz tube at 190 g/min. This corresponds to 0.05 gal/(min)(rod) for a reactor core and is within the design range for ECCS operation. Inductive heating was continued throughout the spray-cooling period.

In test No. 1Z-4, the rod was heated above the melting point of Zircaloy-2 and then sprayed with water for 30 sec. During the quenching period, the rod temperature dropped rapidly from a maximum of 2045 to 1380°C. After the water was turned off, the temperature increased to about 1550°C, at which time the heating coil was deenergized. Crumbling of the fuel rod after cool-down was noted in this test.

In test No. 1Z-5, the fuel rod was heated to simulate a reactor core temperature below the melting point of Zircaloy-2. This rod cooled from 1750 to 110°C in 185 sec. In test No. 1Z-6, the rod was heated to simulate a reactor core temperature well above the Zircaloy-2 melting point. This rod cooled from ~2820 to 95°C in 180 sec. Both rods remained intact during their tests; breakage occurred during their removal from the quartz tube.

The results of these preliminary tests led to the consensus that the degree of fragmentation did not necessarily depend upon the maximum temperature to which the rods were heated. Rather the temperature-time history and embrittlement caused by cladding oxidation are the determining factors; and these two factors are not independent.

3. Parametric Tests of Induction Heated-water Quenched Fuel Rods

The foregoing tests with single Zircaloy-2-clad rods and bundles of four, indicated that the rods retained their original shape at temperatures substantially higher than the melting point of zirconium (1850°C). The tests also indicated that fuel-rod movement or breakup occurred during or after cool-down, with or without water quenching. However, these tests did not reveal the conditions under which gross fragmentation would occur. Accordingly, 18 additional tests were made with single fuel rods to assess the extent of damage and failure of the cladding and fuel as a function of heating rate, steam flowrate, cladding oxidation, quench temperature, quench rate, and method of quench (top or bottom).

Each fuel rod consisted of 0.5-in.-dia UO_2 pellets encased in Zircaloy-2 tubing of 12-in. length, 0.567-in. OD, and 0.031-in. wall thickness. A W5-Re/W26-Re thermocouple was positioned between the fuel pellets and cladding. Each rod was then filled with helium to a pressure

of 10 psig. This assembly was positioned in a 0.865-in.-ID quartz steam jacket such that the thermocouple was near the axial center of the 3-in.-long induction-heating coil that encircled the steam jacket.

During each test, the steam flow was maintained at 2 g/min, and the rod was heated to a predetermined temperature, and then suddenly quenched by admitting water, at room temperature and 190 g/min, either at the top or bottom of the steam jacket (see Fig. 3b). The hydrogen evolved was collected and its volume measured. Posttest metallographic examinations were made of the cladding and the fuel pellets.

To inductively heat a fuel rod to 1000-2100°C at about 5°C/sec and thus simulate loss-of-coolant conditions, heat must be added at a much greater rate than that generated by decay heating in the reactor core. This is because heat losses from a single rod are much greater than from a rod surrounded by other rods in the core. However, when quenching starts, the heat loss to the cooling water from a single rod becomes more nearly equal to the heat loss of a rod in a core being quenched.

Also, it is extremely difficult to determine at what power level the induction heating should be held during the quenching period to simulate the actual conditions experienced by a rod in a reactor core. In some tests, the power level was maintained constant throughout the quenching period. This resulted in adding an unknown amount of energy greater than actually needed. In other tests, the induction generator was turned off when quenching was started; this resulted in adding less energy than needed. Thus, the actual conditions were bracketed.

When the cladding reacts with the steam, releasing hydrogen, part of the oxygen produced dissolves in the cladding and part reacts with the cladding to form ZrO_2. The moles of oxygen produced were considered to be half of the moles of hydrogen collected. The average extent of cladding oxidation (to ZrO_2) as well as the maximum extent of oxidation in any cross section of the 3-in.-long heated section of the rods was estimated from metallographic examination of the rods. Although several layers of different-colored oxides were observed during these examinations, the overall composition of the layers of oxide was assumed to be $ZrO_{2.0}$.

Table III lists the test results in order of increasing average ZrO_2 content of the cladding in the 3-in. heated length. From the differences between the moles of oxygen computed from the hydrogen collected and the moles of ZrO_2 estimated from metallographic examinations, the mole-percent of oxygen dissolved in the unoxidized cladding was estimated. This amount increased with increased amount of metal oxidation. An equivalent average reaction of the 3-in. heated length of cladding was then computed from the total oxygen produced. Rods with equivalent average reactions of ≥ 18.4 mol % failed, whereas those of ≤ 17.0 mol % remained intact. If the

unrestrained rods remained intact on cooling and gentle handling, they were considered not to have failed. It is likely that restraints or rough handling would have lowered the percent of reaction required for failure.

TABLE III. Summary of Parametric Tests of Induction Heated-water Quenched Fuel Rods

Fuel rods: Zircaloy-2-clad UO_2 pellets
Steam flowrate: 2 g/min
Flowrate of cooling water: 190 g/min

Test No.	Heating Rate, °C/sec	Quench Temp, °C	Bottom or Top Quench	Power On or Off during Quench	Hydrogen Collected,[a] mol	ZrO_2 Produced,[b] mol % Avg	ZrO_2 Produced,[b] mol % Max	Apparent Dissolved O_2 in Unoxidized Metal, mol %	Equivalent Average Reaction,[c] mol %	Fuel-rod Condition
12	9.0	1064	Top	On	0.0	1.6	3.2	-	-	Intact
4	4.8	1462	Bottom	Off	0.025	3.5	6.8	3.45	6.87	Intact
7	6.0	1488	Bottom	On	0.026	3.7	6.1	3.6	7.14	Intact
16[d]	~50	1182	Top	On	0.024	3.8	5.4	2.9	6.59	Intact
15	6.4	1548	Top	Off	0.025	4.0	8.0	3.0	6.87	Intact
8	3.1	1534	Bottom	On	0.029	4.8	8.0	3.34	7.97	Intact
9	5.2	1498	Top	On (3.55)[e]	0.042	7.0	12.0	4.88	11.54	Intact
5	5.0	1663	Bottom	Off	0.062	12.3	21.1	5.0	17.03	Intact
17	4.8	1798	Bottom	Off	0.067	14.0	22.0	4.5	18.40	Failed
18	4.6	1569	Top	On (3)[e]	0.068	14.3	22.3	4.5	18.68	Failed
11	5.7	1849	Top	Off	0.081	16.0	22.1	7.3	22.25	Failed
3	4.7	1646	Bottom	On	0.093	13.0	25.0	-	25.55	Failed
10	4.5	1650	Top	Off	0.080	17.6	29.0	5.18	21.98	Failed
6	5.7	1864	Bottom	Off	0.081	17.4	34.5	5.6	22.25	Failed
13	5.1	1663	Top	On (4.18)[e]	0.102	20.5	34.0	9.3	28.02	Failed
14	6.5	2052	Top	On (2.75)[e]	0.14	30.0	41.0	12.0	38.46	Failed
1	6.3	2110	Top	On	>0.1	-	~100	-	-	Failed
2	5.2	1868	Top	On	>0.1	-	~100	-	-	Failed

[a]Oxygen produced was taken to be half this amount.
[b]From metallurgical examination of 3-in. heated length of cladding.
[c]Equivalent average reaction of 3-in. heated length of cladding based on total oxygen produced.
[d]This run followed a predetermined temperature-time curve simulating a particular ECC (emergency core-cooling) situation (see text).
[e]Power turned off at this time (min) after start of quench.

The cladding temperature-time relationship employed in test No. 16 was taken from calculations for a postulated emergency core-cooling (ECC) case. This relationship was maintained throughout the heat-up and quench stages by adjusting the induction-heating power as required. The temperature was initially increased at a rapid rate (~50°C/sec), held near 1182°C for 9 min, and then decreased rapidly. Top quenching was started 0.5 min after the temperature reached 1182°C and was continued for about 8.5 min (until the temperature decreased).

Table IV shows the failure pattern of the claddings as a function of quench temperature in instances where the heating power was continued or discontinued after quenching was initiated from the top or bottom of the steam jacket. The quench temperatures listed are the maximum temperatures attained by the cladding at the time quenching was initiated. As

shown in Table IV, the lowest temperatures at which cladding failure was observed occurred in tests in which heating power was continued after top quenching was initiated.

TABLE IV. Failure Pattern of Inductively-heated Single Zircaloy-2-clad Fuel Rods

Quench Temp, °C	Power On after Quench Initiated		Power Off after Quench Initiated	
	Top Quench	Bottom Quench	Top Quench	Bottom Quench
1064	I[a]			
1182	I			
1462 to 1498	I	I		I
1534 to 1569	F[b]	I	I	
1646 to 1663	F	F	F	I
1798				F
1849 to 1868	F		F	F
2050 to 2110	F			

[a] I indicates that fuel rod remained intact.
[b] F indicates that fuel rod failed.

An evaluation of these test results must take into account the fact that the fuel rods were only 12 in. long, with a 3-in.-long heated section, and were not mechanically restrained in the test assembly. Embrittlement and loss of strength of the cladding increase with the degree of cladding oxidation, oxygen dissolved in the cladding, and interaction of the cladding with the UO_2. Therefore, the unrestrained fuel rods that did not fail in these tests might have failed if subjected to the restraints and warpage that could occur in bundles of fuel rods in a reactor core. In addition, the efficiency of cooling the latter rods may be considerably different from that of cooling single rods. Finally, the effects of nuclear radiation, methods of heating (decay versus induction), and gas pressure in the rods also may reflect changes in the results.

Nevertheless, for the conditions prevailing in these tests, the critical quench temperature for unrestrained fuel-rod failure would be in the range from 1500 to 1700°C. (See Table IV.) For fuel rods subjected to emergency-cooling conditions (loss-of-coolant accident) in a water-cooled power reactor, the maximum rod temperatures are estimated to range from 1000 to 1200°C.

Upon completion of each test, the rod was carefully removed from the steam jacket and photographed immediately. In Fig. 18, the rods are displayed in order of increasing cladding oxidation. The corresponding test conditions and data are listed in Table III. It is apparent that as the oxidation increased, the oxide exhibited an increasingly whiter appearance.

Rods from tests No. 12, 4, 7, 16, 5, 8, 9, and 5 remained intact after photographing and during sectioning for metallographic examination. The rod in test No. 16 was slightly bowed; this was apparently due to high-temperature gradients caused by the rapid heating rate (50°C/sec) and the water quench. Each of the other rods broke either during cooling (No. 3, 14, 1, and 2) or on handling preparatory to sectioning (No. 17, 12, 11, 10, 6, and 13). Sectioning revealed some internal cracks in the cladding which were not visible externally.

The thin (~1-2 mil) layer of oxide flaking from rods in tests No. 7, 15, 8, 18, and 3 is attributed to thermal shock during the quenching phase. Because of its thinness, the flaking did not appreciably weaken the rods.

Figure 19 shows typical photomacrographs of horizontal cross sections cut through the cladding at 0.5-in. intervals, starting from the midpoint of the 3-in.-long heated section. Where appearing, the dark gray areas are the zirconium oxide, and the light areas are the Zircaloy-2 cladding. The black areas are either the potting compound or holes in the surface. The cladding and oxide were very brittle, and during polishing, pieces were lost, leaving holes.

Hansen and Anderko's[12] phase diagram for zirconium-oxygen shows that the alpha-beta transition in zirconium is appreciably increased by dissolved oxygen. Maximum oxygen solubility is given as 29.2 at. %. A transition temperature of ~1000°C for ZrO_2 from tetragonal to monoclinic crystal structure is also given. These transitions, particularly in the case of ZrO_2, are apparently largely responsible for the cracking that occurred on cooling of the test fuel rods. Hansen and Anderko report that, at least above 700°C, evidence of oxides lower than ZrO_2 is lacking.

4. Effects of Hydriding

During a reactor loss-of-coolant accident, steam flowing upward through the core could oxidize the fuel cladding in the lower half of the core, thereby producing a hydrogen atmosphere (containing more or less steam) in the upper half. Accordingly, five scoping tests (No. H1 to H5) were made with single, inductively heated, Zircaloy-2-clad rods to determine the relative cladding damage due to hydriding as compared to oxidation.

Fig. 18. Induction Heated-water Quenched Zircaloy-2-clad Fuel Rods in Order of Increasing Cladding Oxidation (see Table III)

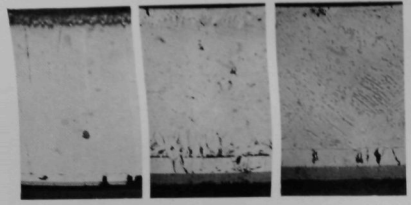

(a) (b) (c)

TEST NO. 4. (a) 1 in. below mid-point; (b) 0.5 in. below mid-point; (c) at mid-point.

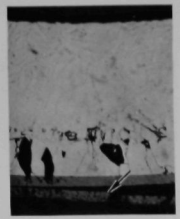

TEST NO. 8. Arrow points to flaking of oxide from cladding at mid-point.

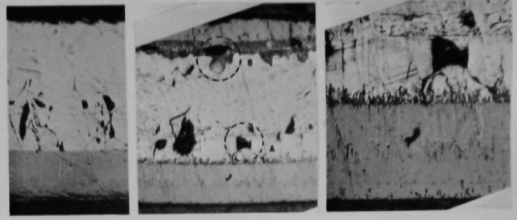

(a) (b) (c)

TEST NO. 5. (a) Mid-point; (b) 0.5 in. below mid-point; (c) enlargement of inset A.

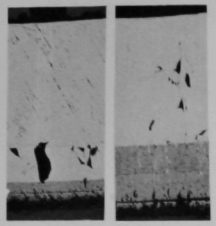

(a) (b)

TEST NO. 18. (a) 1 in. and (b) 0.5 in. below mid-point.

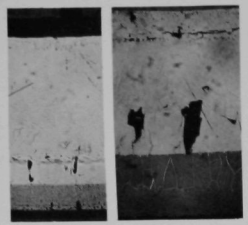

(a) (b)

TEST NO. 11. (a) 1 in. below mid-point; (b) at mid-point.

TEST NO. 3. (TOP) Interior cladding surface oxidized by entry of steam; (BOTTOM) Flaking of oxide from outer surface; 0.5 in. below mid-point.

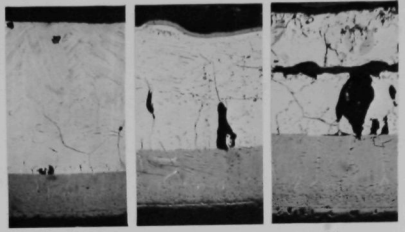

(a) (b) (c)

TEST NO. 10. (a) 1 in. below and (b) 0.5 in. below midpoint; (c) at mid-point.

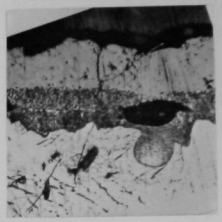

(d)

Enlargement of inset B, TEST NO. 5 above, showing reaction between Zircaloy-2 and UO_2.

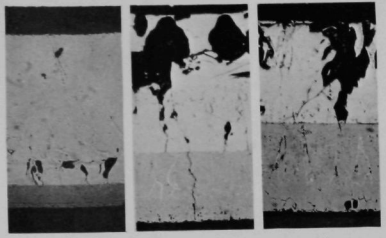

(a) (b) (c)

TEST NO. 6. Increased oxidation from (a) 1 in. and (b) 0.5 in. below mid-point, to (c) at mid-point.

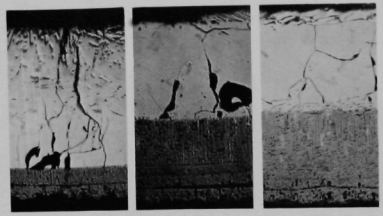

(a) (b) (c)

TEST NO. 13. (a) 1 in. and (b) 0.5 in below mid-point; (c) at mid-point.

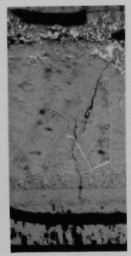

TEST NO. 1. Eight layers of cladding oxide at mid-point.

TEST NO. 2. Arrow points to oxidation along crack 1.5 in. below mid-point.

Fig. 19. Selected Horizontal Cross Sections of Cladding Cut from Midpoint and Levels below Midpoint of Heated 3-in.-long Section of Zircaloy-2-clad Fuel Rods Exposed in Parametric Tests. Rods displayed in order of increasing cladding oxidation (see Table III). Cladding thickness = 0.031 in.; outer surface at bottom, inner surface at top.

Each rod was identical in composition and dimensions to those used in the parametric tests. Cladding temperature was measured at the midpoint of the 3-in.-long heated section of the rod. This section of the cladding contained about 16.67 g or 0.182 mole of zirconium. The amount of hydrogen absorbed was measured in all but test No. H2.

Hansen and Anderko[12] have reported that the equilibrium solubility of hydrogen in zirconium decreases as the temperature is increased; however, at low temperatures, the kinetics or rates of solution are very low. Thus, when Zircaloy-2 cladding is heated in hydrogen for a given period of time at various temperatures, maximum hydriding may occur at some intermediate temperature. This occurred in the current tests.

The test conditions and results are summarized in Table V. In tests No. H1 and H3, the rods were heated and maintained at 1650°C for 9 min and 1400°C for 6 min, respectively, in a hydrogen atmosphere. In test No. H2, the rod was held at 1400°C for 6 min in a flowing atmosphere of 50% hydrogen-50% steam. In test No. H4, the rod was preoxidized at 1100°C for 7 min in steam flowing at 2 g/min; it was then heated at 1400°C for 6 min in a hydrogen atmosphere. In test No. H5, the rod was preoxidized at 1100°C for 6 min in steam at the same flowrate, and then heated at 1500°C for 6 min in a hydrogen atmosphere.

TABLE V. Summary of Hydriding Scoping Tests of Single Zircaloy-2-clad Fuel Rods

Cladding density (mol wt = 91.2): 6.5 g/cm^3
ZrO_2 density (mol wt = 123.2): 5.7 g/cm^3

Test No.	Temp, °C	Time at Temp, min	Ambient Gas	Cladding				
				H_2 Absorbed		Oxidation, %		Posttest Condition
				moles	at. %, avg	Max	Avg	
H1	1650	9	H_2	0.049	34	-	-	Failed near ends of heated section
H2	1400	6	H_2-H_2O	-	-	9.7	6.1	Intact
H3	1400	6	H_2	0.016	15	-	-	Intact
H4	1400	6	H_2	0.0018	2	~2	~1.5	Intact
H5	1500	6	H_2	0.00805	8	~2	~1.5	Intact

Figure 20 shows the rods as photographed immediately upon their removal from the quartz jacket.

Metallographic examination of cross sections taken from various levels along the 3-in. heated length revealed only slight hydride embrittlement near the axial center of the rods in tests No. H3, H4, and H5 (see Fig. 21). The rod in test No. H2 evidenced some oxidation due to the presence of steam. Three cross sections cut from the rod in test No. H1 showed (1) some hydride near the axial center, (2) reaction between

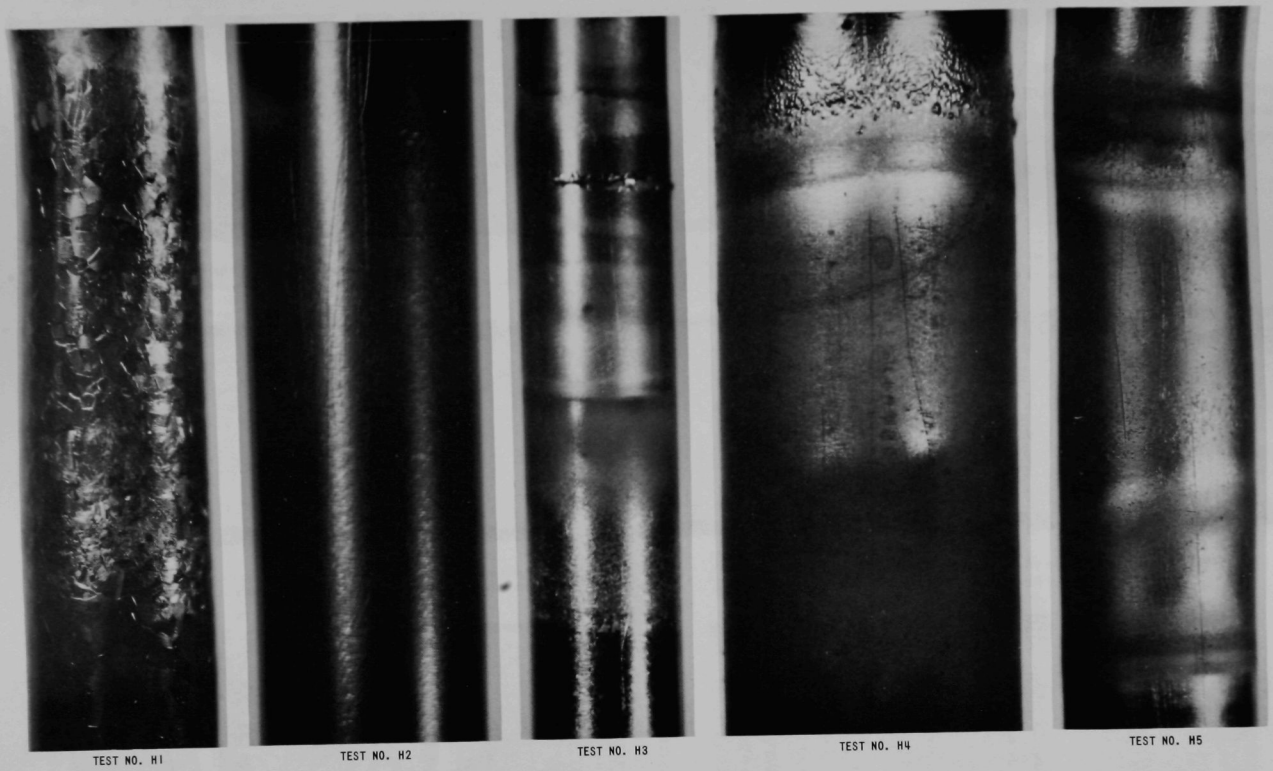

Fig. 20. Heated Sections of Zircaloy-2-clad Fuel Rods Exposed to Hydrogen and Hydrogen-Steam Atmospheres in Tests No. H1 to H5 (see Table V)

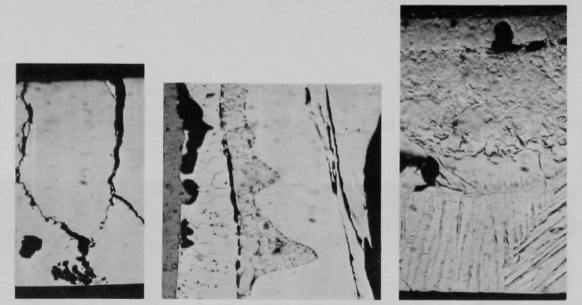

(a) (b) (c)

TEST NO. H1. (a) Severe hydriding and embrittlement of cladding 1.5 in. below mid-point; (b) reaction between cladding and UO_2 0.5 in. below mid-point; (c) moderate hydriding at mid-point.

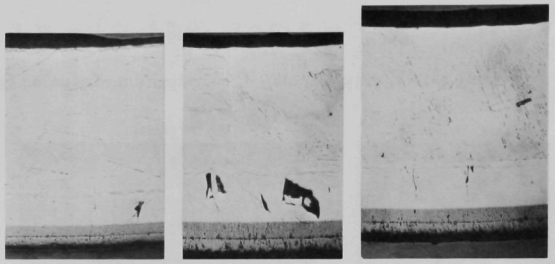

(a) (b) (c)

TEST NO. H2. Oxidation and very mild hydriding of cladding in 50% steam-50% hydrogen atmosphere (a) 1 in. and (b) 1.5 in. below mid-point; (c) at mid-point. Oxidation is clearly visible and dominant.

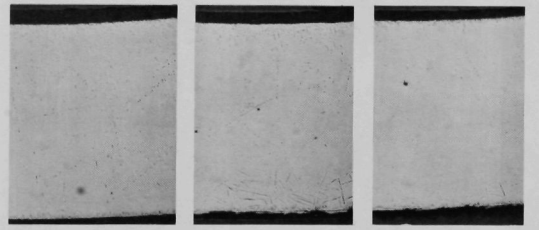

(a) (b) (c)

TEST NO. H3. Considerable hydriding of cladding (a) 1 in. and (b) 1.5 in. below mid-point, and (c) at mid-point. Maximum hydriding occurred at (b).

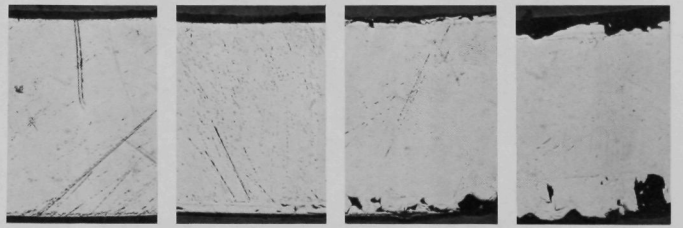

(a) (b) (c) (d)

TEST NO. H4. Moderate hydriding and oxidation (a) 1.5 in., (b) 1 in., (c) 0.5 in. below mid-point, and (d) at mid-point. Cladding was pre-oxidized in steam. Both oxide and hydride are visible. Eroded edges in (c) and (d) were caused by polishing.

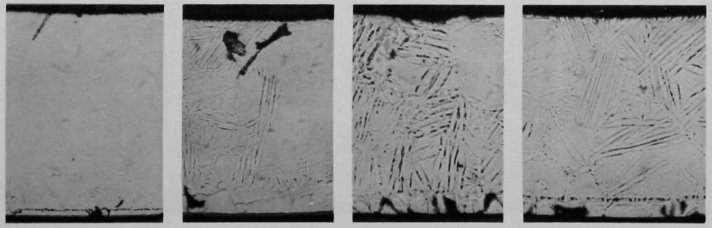

(a) (b) (c) (d)

TEST NO. H5. Increasing hydrogen embrittlement of cladding (a) 1.5 in., (b) 1 in., (c) 0.5 in. below mid-point, and (d) at mid-point. Cladding was pre-oxidized in steam. Both oxide and hydride are visible.

Fig. 21

Selected Horizontal Cross Sections of Cladding Cut from Mid-point and Levels below Midpoint of Heated 3-in.-long Section of Zircaloy-2-clad Fuel Rods Exposed in Tests No. H1 to H5 (see Table V). Cladding thickness = 0.031 in.; outer surface at bottom, inner surface at top.

the cladding and UO_2 at a level 0.5 in. below the axial center, and (3) severe hydriding and embrittlement of the cladding near the lower end of the heating coil. The latter cross section was in a region of relatively lower temperature.

The results of these scoping tests indicate that:

(1) Less hydriding damage is incurred in Zircaloy-2 cladding exposed for 6-9 min to a hydrogen atmosphere at 1400-1650°C than is incurred by oxidation in steam at the same temperature range and period of exposure.

(2) The presence of steam in hydrogen, or preoxidation of the Zircaloy-2 cladding, greatly reduces the hydriding effects.

V. CONCLUSIONS

1. When oxidized by heating in a steam atmosphere, Type 304 stainless steel cladding foams and expands at temperatures approaching its melting point (~1400°C).

2. Zircaloy-2 cladding (~0.030 in. thick), which has a melting point of ~1850°C, did not run or drip from UO_2 fuel pellets at temperatures as high as 2140°C.

3. Partially-oxidized Zircaloy-2 cladding around UO_2 fuel pellets forms an oxide shell which can retain segments of molten metal at temperatures in the range 2600 to 2800°C.

4. Zircaloy-2 metal that has absorbed oxygen is embrittled, and the degree of embrittlement increases with the amount of oxygen absorbed.

5. Oxidation of Zircaloy-2 cladding in an excess-steam atmosphere follows the parabolic rate law for zirconium.[10] In a limited-steam atmosphere, the oxidation rate may be diminished by diffusion of steam through the hydrogen product to the surface.

6. Zircaloy-2 oxide has a tendency to crack and break on cooling after prolonged exposure to steam at temperatures above 1200°C. At room temperature, the oxide is very brittle. The tendency to break on cooling is due to a phase change in ZrO_2, from tetragonal to monoclinic crystal structure, at about 1000°C.[12]

7. Zircaloy-2-clad, UO_2-pellet fuel rods can be heated to about 1200°C in a steam atmosphere and then water-quenched for about 6 min without incurring sufficient oxidation and embrittlement to break on cooling.

8. When unrestrained Zircaloy-2-clad fuel rods are heated at ~5°C/sec in a dynamic steam atmosphere, the critical quench temperature range is 1500 to 1700°C. At lower heating rates, prolonged oxidation would cause the rods to fail at lower quench temperatures.

9. The major factor in Zircaloy-2 cladding failure due to steam oxidation embrittlement and water quenching is the extent of oxidation. This extent, in turn, is influenced by the cladding temperature and the time at temperature. When the equivalent reaction as ZrO_2 (based on total oxygen absorbed) is ≥18%, the cladding becomes very brittle. When it is <10%, the cladding retains a fair amount of strength.

10. When exposed for 6 min or longer to a pure hydrogen atmosphere at 1400°C, Zircaloy-2 cladding is embrittled due to hydriding. Preoxidation of the cladding in steam, or the presence of steam in the hydrogen, reduces the degree of hydrogen embrittlement. However, conditions that might produce sufficient hydrogen embrittlement of the cladding in one region of a reactor core would cause much greater embrittlement due to oxidation in other regions. Thus the effects of hydriding are secondary to those of oxidation.

REFERENCES

1. *Chemical Engineering Division Semiannual Report, January–June 1964*, ANL-6900, p. 243 (Aug 1964).

2. Ibid., *July–December 1964*, ANL-6925, p. 187 (May 1965).

3. Ibid., *January–June 1965*, ANL-7055, p. 192 (Oct 1965).

4. Ibid., *July–December 1965*, ANL-7125, pp. 150-153 (May 1966).

5. Ibid., *January–June 1966*, ANL-7225, p. 164 (Nov 1966).

6. Ibid., *July–December 1966*, ANL-7325, p. 142 (April 1967).

7. Ibid., *January–June 1967*, ANL-7375, p. 144 (Oct 1967).

8. B. Lustman, *Zirconium-Water Reaction Data and Application to PWR Loss-of-Coolant Accident*, WAPD-SC-543 (May 1957).

9. J. I. Owens *et al.*, *Metal-Water Reactions: VIII. Preliminary Consideration of the Effects of a Zircaloy-Water Reaction during a Loss-of-Coolant Accident in a Nuclear Reactor*, GEAP-3279 (Sept 1959).

10. L. Baker, Jr., and L. C. Just, *Studies of Metal-Water Reactions at High Temperatures: III. Experimental and Theoretical Studies of the Zirconium-Water Reaction*, ANL-6548 (May 1962).

11. *Physico-Chemical Studies of Clad UO_2 in Potential Meltdown Environments in High-Temperature Materials Program Progress Report No. 58, Part A*, GEMP-58A, p. 55 (April 29, 1966).

12. M. Hansen and K. Anderko, *Constitution of Binary Alloys*, 2nd ed, McGraw-Hill Book Co., Inc., New York, p. 1078 (1958).